COMPARISON OF DIELECTRIC SURFACE PASSIVATION OF MONOCRYSTALLINE AND MULTICRYSTALLINE SILICON

Jed Brody and Ajeet Rohatgi
Georgia Institute of Technology, Atlanta, GA 30332-0250

ABSTRACT

Reducing solar cell thickness is an attractive way to reduce material costs. However, model calculations in this paper show that if rear surface recombination velocity (S) is greater than about 1000 cm/s, a 100-μm-thick screen-printed cell on solar-grade material has a lower efficiency than a 300-μm-thick cell. The literature demonstrates that S < 1000 cm/s is readily achievable on monocrystalline materials. However, S on multicrystalline silicon (mc-Si) seems less thoroughly investigated. In this study, string ribbon mc-Si wafers of different resistivities are passivated with a thermal oxide, plasma-enhanced chemical vapor deposition (PECVD) nitride, and an oxide/nitride stack. For comparison, float zone (FZ) and Czochralski (Cz) monocrystalline wafers are passivated identically. By analyzing measured lifetimes under 500 nm and 1000 nm illumination, upper and lower limits on S are determined. For most of the monocrystalline wafers investigated in this study, the upper limit on S is less than 1000 cm/s, while for most of the multricrystalline wafers, 1000 cm/s falls within the error bars. Thus, thinning monocrystalline silicon should improve cell performance; however, it is difficult to conclude from this data that solar cell efficiency will improve when reducing thickness for the specified mc-Si materials and passivation technologies. In fact, results strongly suggest that S on string ribbon mc-Si is higher than S on identically passivated FZ.

INTRODUCTION

About 40-50% of the cost of a photovoltaic module is associated with silicon material growth and wafering [1]. Thus, in order to lower the cost of silicon solar cells, reduction in cell thickness is being actively investigated [1, 2]. One challenge facing manufacturers of thin solar cells is rear surface passivation, because implementation of the standard aluminum back surface field (Al BSF) can cause thin wafers (≤ 150 μm) to warp, resulting in unacceptable yield [3]. Accordingly, dielectric rear passivation is being pursued [4]. While dielectric passivation has been used to achieve surface recombination velocity (S) as low as 4 cm/s on 1.5 Ω-cm monocrystalline substrates [5], it is unclear whether the same dielectric can passivate the multicrystalline silicon surface as effectively as the monocrystalline surface; defects like grain boundaries and dislocations at the multicrystalline silicon/dielectric interface may affect passivation. Since S may be different on identically processed monocrystalline and multicrystalline silicon, S values measured on monocrystalline silicon should not be used when modeling multicrystalline devices. If small S is assumed, modeling indicates that reducing cell thickness (W) from 300 μm to 100 μm improves efficiency [2], whereas the opposite is true if S is high. This is demonstrated by the simulation results of Fig. 1: for a bulk lifetime (τ_b) of 20 μs, approximately 1000 cm/s is the S value below which thinner cells are superior and above which thicker cells are superior. It has been experimentally verified that efficiency improves as BSF cells are thinned, whereas efficiency decreases when cells with poorly passivated rear surfaces are thinned [6]. Thus when considering thickness reductions of multicrystalline devices in order to reduce material costs, one must know S well enough to determine whether efficiency will improve or decline with decreasing thickness.

This paper presents the results of measurements of spatially averaged S on dielectric-passivated string ribbon using quasi-steady-state photoconductance. In order to determine S, the contributions of both S and τ_b to the effective lifetime (τ_{eff}) must be separated. Every known method for suppressing S to determine τ_b has its drawbacks, as described in [7]. Additionally, we recently showed [8] that while an iodine/methanol solution [9] reliably passivates the monocrystalline silicon surface more effectively than the dielectrics under investigation, the string ribbon silicon surface is often less effectively passivated by the iodine/methanol solution than the dielectrics. Thus, the iodine/methanol solution cannot be used to suppress S for the separation of surface and bulk recombination in materials like string ribbon silicon.

Given the failure of the iodine/methanol solution to determine τ_b accurately enough to calculate S on string ribbon silicon, we choose the method described in [10]: two illuminating spectra are used to measure τ_{eff}. Assuming ±10% uncertainty in τ_{eff} measured with each spectrum, we find a region in the S-τ_b plane consistent with each measurement. The intersection of the regions given by the two τ_{eff} measurements provides a range of S and τ_b values consistent with the two measurements. Figure 2 illustrates the determination of S on a nitride-passivated string ribbon wafer. The region bounded by the solid lines is consistent with τ_{eff} measured using 500 nm illumination, and the region bounded by the broken lines is consistent with τ_{eff} measured using 1000 nm illumination; the intersection thus gives the region in the S-τ_b plane consistent with both measurements. In this case, 390 cm/s < S < 4500 cm/s. Using this method, we proceed to determine S on dielectric-passivated monocrystalline and multicrystalline silicon.

EXPERIMENTAL DETAILS

Three kinds of silicon materials were selected: FZ of 0.7 Ω-cm, 1.3 Ω-cm, and 2.9 Ω-cm resistivity; Cz of 1.2 Ω-cm, 1.6 Ω-cm, and 4.7 Ω-cm resistivity; and Evergreen string ribbon of 0.7 Ω-cm, 1.5 Ω-cm, and 3.0 Ω-cm resistivity. The wafers were cleaned in standard chemical solutions. Subsequently, a wafer of each type was processed in one of the following three ways:

A. Stack passivation: 100 Å thermal oxide grown at 925°C in a tube furnace followed by deposition at 300°C of 850 Å high-frequency, direct PECVD nitride on both sides.

B. Oxide passivation: 100 Å thermal oxide only.

C. Nitride passivation: 850 Å PECVD nitride only.

All wafers received a 20 minute forming gas anneal at 400°C. τ_{eff} was measured under both 500 nm and 1000 nm illumination. This illumination was achieved by using monochromatic optical filters with bandwidths of 71 nm and 16 nm, respectively. The lifetime measurements were analyzed to extract S ranges according to the method introduced in [10], elaborated in [8], and illustrated in Fig. 2. Since the inductive coil used to measure photoconductance is larger than a single grain, this technique gives a spatially averaged S. As in Fig. 2, we estimated an error of ±10% in computed τ_{eff} values to accommodate uncertainty in measured wafer thickness, reflectance, resistivity, and reference cell spectral response. For the string ribbon wafers, an τ_{eff} error of ±5% was also used for comparison.

Each wafer had a different range of injection levels accessible to measurement, due to non-recombinative trapping [11] and the optical filters. Thus, it was not possible to measure τ_{eff} at the same injection level on each wafer. The injection levels at which τ_{eff} was measured range from 5×10^{13}-2×10^{15} cm^{-3}, with as similar as possible injection levels chosen for all wafers of a given material.

RESULTS AND DISCUSSION

Figure 3 shows the results for FZ. This material was processed along with the others as a control, since the surface passivation of FZ is well described in the literature [12]. While the iodine/methanol method [9] could have been used on FZ, the two-spectrum method was used instead for consistency. As expected, Fig. 3 indicates that S on all but one wafer is well under 500 cm/s. Figure 3 supports the trend that S declines as resistivity increases. In most cases, this trend is predicted and confirmed [12]. Figure 4 summarizes the results on the Cz material. With the exception of the 1.6 Ω-cm wafers, results are comparable to those of FZ and indicate S less than 600 cm/s. The cause for the anomalous results for the 1.6 Ω-cm wafers is unclear; small errors in measured thickness, reflectance, and resistivity can all substantially influence the results [8]. Another possibility is that the 1.6 Ω-cm wafers came from a defective batch.

Figure 5 shows the results for a single point measured on each string ribbon wafer. Since the material is spatially non-uniform, measurements on other points gave different results, but not dramatically altered trends. In Fig. 5, the shading indicates the S ranges obtained for two different uncertainties in τ_{eff}: the dark segments correspond with ±5% in the measured τ_{eff} values, and the entire columns correspond with ±10%. For ±10% error, the S range indicated for string ribbon extends about an order of magnitude higher than that of FZ of similar resistivity. For example, S for oxide-passivated string ribbon may be as high as 2700 cm/s on 0.7 Ω-cm material, 2200 cm/s on 1.5 Ω-cm material, and 540 cm/s on 3 Ω-cm material; maximum S values for oxide-passivated FZ of similar resistivity were found to be 180 cm/s, 58 cm/s, and 94 cm/s (Fig. 3). Thus, while S on FZ may easily be guaranteed to be less than 1000 cm/s, S on identically passivated string ribbon is not certain to be as low. Consequently, these results cannot predict whether reducing the thickness of string ribbon solar cells will improve efficiency, as illustrated in Fig. 1.

Even when lowering the estimated uncertainty to ±5%, all of the string ribbon samples have upper S limits that exceed 1000 cm/s. Moreover, measurements on the oxide-passivated 3.0 Ω-cm wafer cannot be analyzed when uncertainty is only ±5%: then there is no intersection in the S-τ_b plane between the region consistent with the 500 nm measurement and the region consistent with the 1000 nm measurement. Thus, at least one of the τ_{eff} values measured on this wafer must be more than 5% away from the true value. In fact, after repeating a τ_{eff} measurement 20 times and performing the calibration procedure described in [8] before each measurement, we find a 10% standard deviation in the distribution of τ_{eff} values. Thus, the technique as currently practiced cannot yield results with higher precision than those of Figs. 3-5.

A comparison of dielectrics on FZ confirms that high-frequency direct nitride alone is not as effective as stack passivation or a thermal oxide; for a given resistivity, the upper limit on S for a nitride is at least double that for stack or oxide. On string ribbon, however, this trend appears weakened, with the upper limit on S for nitride usually no more than 150% that for stack or oxide on the same resistivity. It may be that defects in string ribbon reduce the dependence of surface quality on dielectric type.

CONCLUSIONS AND FUTURE WORK

Thinning wafers to reduce cost may have the undesired consequence of reducing efficiency unless rear S is sufficiently low. For a wafer with τ_b = 20 μs, S must be less than about 1000 cm/s in order for a 100-μm-thick solar cell to perform better than a 300 μm cell. While adequately low S values are easily achievable on FZ wafers, S for identically passivated mc-Si is not necessarily as low. Experimental results obtained using the two-

spectrum technique indicate that the upper limit on spatially averaged S for string ribbon silicon is an order of magnitude higher than the upper limit on S for identically passivated FZ. The upper limit on S for most of the monocrystalline wafers investigated in this study was less than 1000 cm/s, while the upper limit on S for most of the string ribbon wafers exceeded 1000 cm/s. Therefore, it cannot be concluded from this data that reducing thickness would improve efficiency when using the specified multicrystalline materials and passivation technologies. In order to help resolve the ambiguities arising from the wide S ranges obtained, a Monte Carlo analysis under development will assign probabilities to S being greater or less than specified values.

REFERENCES

[1] J. Szlufcik, S. Sivoththaman, J. F. Nijs, R. P. Mertens, and R. van Overstraeten, "Low-cost industrial technologies of crystalline silicon solar cells," *Proc. IEEE* **85**, 1997, pp. 711-730.

[2] A. Rohatgi, A. Ebong, V. Yelundur, and A. Ristow, "Rapid thermal processing of next generation silicon solar cells," *Tenth International Workshop on the Physics of Semiconductor Devices*,1999, pp. 14-18.

[3] A. Schneider *et al.*, "Al BSF for thin screenprinted multicrystalline Si solar cells," *Seventeenth EU-PVSEC*, 2001.

[4] A. Aberle, W. Warta, J. Knobloch, and B. Voss, "Surface passivation of high efficiency silicon solar cells," *Twenty-first IEEE PVSC*, 1990, pp. 233-238.

[5] T. Lauinger, J. Schmidt, A. Aberle, and R. Hezel, "Recond low surface recombination velocities on 1 Ω-cm p-silicon using remote plasma silicon nitride passivation," *Appl. Phys. Lett.* **68**, 1996, pp. 1232-1234.

[6] T. Koval, J. Wohlegemuth, and B. Kinsey, "Dependence of cell performance on wafer thickness for BSF and non-BSF cells," *Twenty-fifth IEEE PVSC*, 1996, pp. 505-507.

[7] H. Schulenburg and H. Tributsch, "Electropassivation of silicon and bulk lifetime determination with dry polymer contact," *J. Phys. D.* **33**, 2000, pp. 851-858.

[8] J. Brody and A. Rohatgi, "Sensitivity analysis of two-spectrum separation of surface and bulk components of minority carrier lifetime," *Solid-State Electronics* **46**, 2002, pp. 859-866.

[9] H. M'Saad, J. Michel , J. J. Lappe, L. C. Kimerling, "Electronic passivation of silicon surfaces by halogens, *J. Electronic Mat.* **23**, 1994, pp. 487-491.

[10] M. Bail and R. Brendel, "Separation of bulk and surface recombination by steady state photoconductance measurements," *Sixteenth European PV Conference*, 2000.

[11] D. Macdonald, R. A. Sinton, and A. Cuevas, "On the use of a bias-light correction for trapping effects in photoconductance-based lifetime measurements of silicon," *J. Appl. Phys.* **89**, 2001, pp. 2772-2778.

[12] A. G. Aberle, *Crystalline Silicon Solar Cells: Advanced Surface Passivation and Analysis*. Sydney, Australia: Centre for Photovoltaic Engineering, University of New South Wales, 1999.

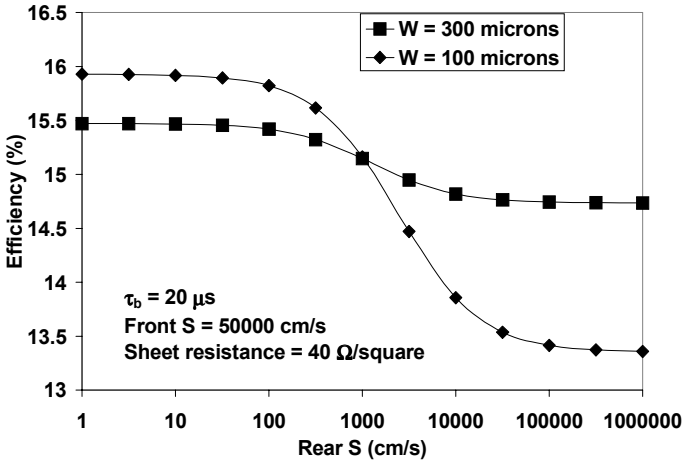

Fig. 1. Simulation demonstrating that thinner cells perform better for S < 1000 cm/s, whereas thicker cells perform better for S > 1000 cm/s.

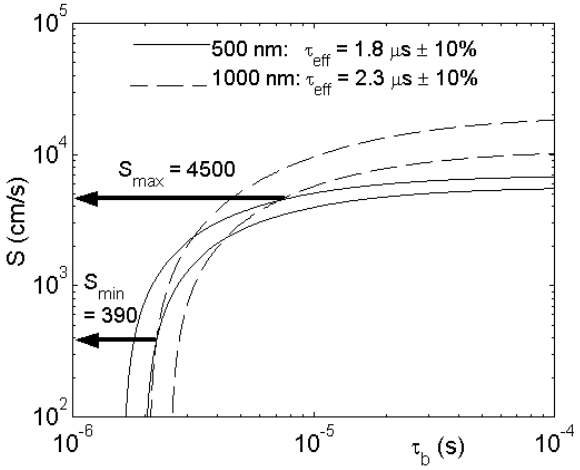

Fig. 2. Illustration of the method of extraction of S values consistent with τ_{eff} measurements under each of two illuminating wavelengths.

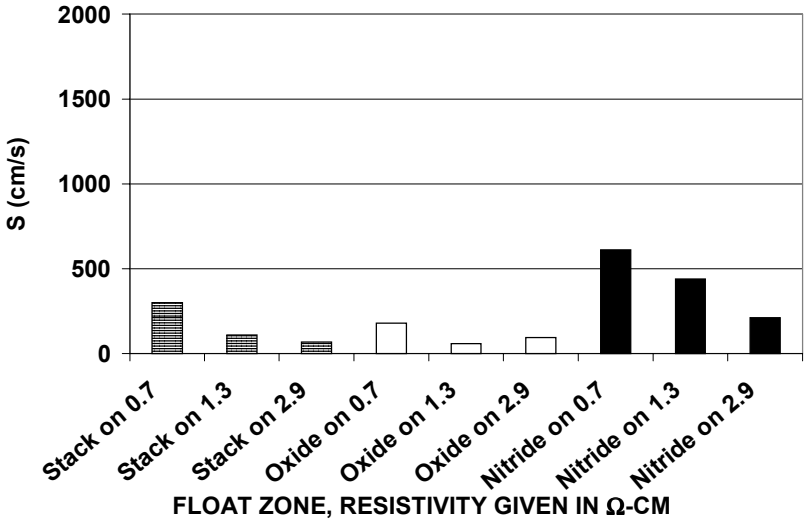

Fig. 3. S ranges determined on float zone. The columns are to be considered error bars spanning the range of S values consistent with τ_{eff} measurements under 500 nm and 1000 nm illumination.

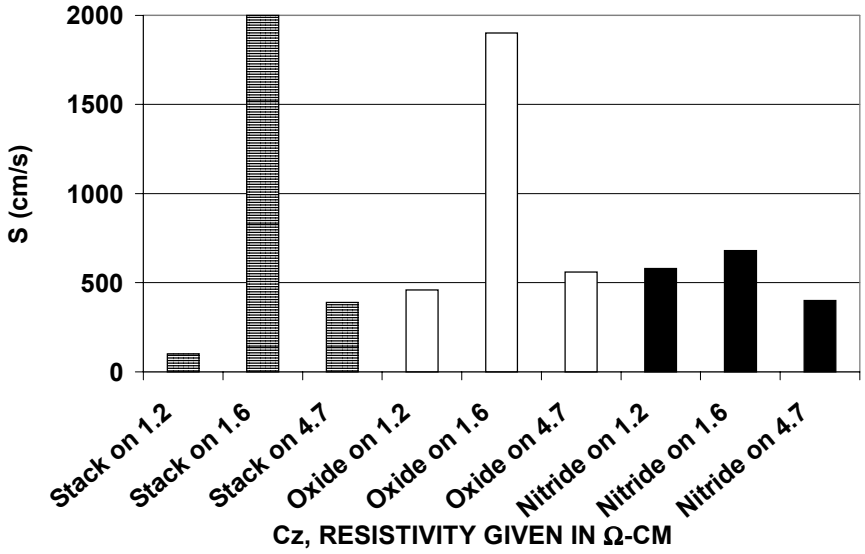

Fig. 4. S ranges determined on Cz.

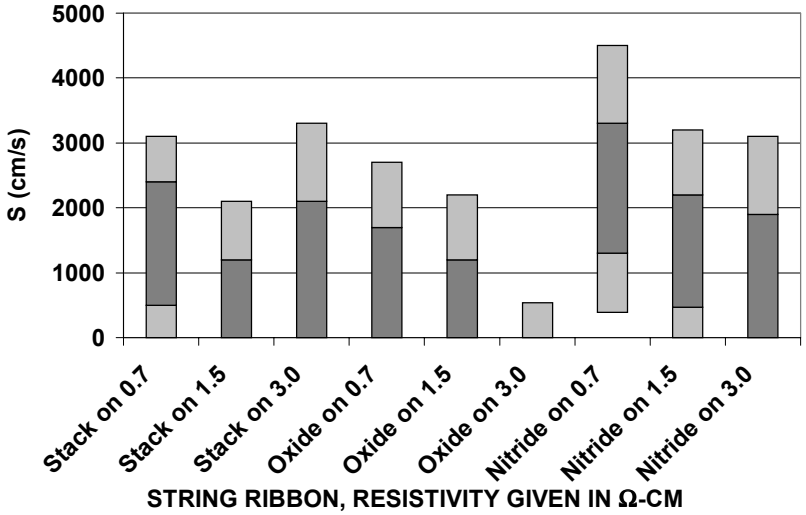

Fig. 5. S ranges determined on string ribbon. The change in scale reflects the higher upper limits relative to the monocrystalline materials. The dark segments represent ±5% in measured τ_{eff}, and the entire columns represent ±10%.